Proc. Natl. Acad. Sci. USA
Vol. 91, pp. 6604–6608, July 1994
Chemistry

The Fenton oxidation mechanism: Reactivities of biologically relevant substrates with two oxidizing intermediates differ from those predicted for the hydroxyl radical

DAVID A. WINK*, RAYMOND W. NIMS*, JOSEPH E. SAAVEDRA*, WILLIAM E. UTERMAHLEN, JR.†, AND PETER C. FORD‡

*Chemistry Section, Laboratory of Comparative Carcinogenesis, National Cancer Institute, Frederick Cancer Research and Development Center, Frederick, MD 21702; †PRI/DynCorp, Frederick Cancer Research and Development Center, Frederick, MD 21702; and ‡Department of Chemistry, University of California, Santa Barbara, CA 93106

Communicated by Ralph G. Pearson, March 17, 1994 (received for review December 6, 1993)

ABSTRACT **The application of kinetic probes that allow one to determine relative reactivities of biologically relevant substrates with oxidizing intermediates in the Fenton reagent (H_2O_2 plus Fe^{2+} in acidic aqueous solution) is described. These results lead to the conclusion that there are two key intermediates with very different reactivity patterns. One (X) is proposed to be an iron complex formed via direct reaction of H_2O_2 with Fe^{2+}, which reacts with *N*-nitrosodimethylamine to generate a strong transient absorption at 450 nm. This provides a sensitive spectrophotometric probe of the competitive reactivities toward X of biologically relevant substrates such as nucleic acid components and amino acids. The second intermediate (Y) is probed by its oxidation of the $Ru(bpy)_3^{2+}$ ion (bpy = 2,2′-bipyridine) to a product with an absorption band centered at 500 nm. In the absence of other substrates, $Ru(bpy)_3^{2+}$ is oxidized at rates independent of the Ru concentration, but the product yield is diminished by competing reactions with substrates that can intercept X. Competition studies demonstrate reactivity patterns for X and Y that are clearly distinct from the pattern predicted for the hydroxyl radical, the intermediate commonly invoked in discussions of Fenton oxidations. These data require reevaluation of the mechanisms by which the Fenton reagent oxidizes biological substrates.**

The powerful oxidant formed from ferrous salts plus H_2O_2 in acidic aqueous solution, first described by Fenton a century ago (1), is often cited as a model for biological processes such as *in vivo* oxidative damage during certain disease states, carcinogenesis, drug-associated toxicity, and postischemic reperfusion injury (2–5). The hydroxyl radical (·OH) is generally invoked as the primary intermediate of such aqueous oxidations (6), although other intermediates have been proposed for related reactions involving chelated iron(II) (7–15). Here we describe applications of additional probes of the reactivities of key Fenton reagent intermediates in aqueous media and resulting data, which argue for reconsidering the mechanisms of these oxidations.

One such probe is the strong, visible-range, transient absorbance (Abs(A)) that is generated when *N*-nitrosodimethylamine (NDMA) reacts with an intermediate (X) formed by the simple reaction of aqueous Fe^{2+} with H_2O_2 in acidic aqueous solution. Earlier kinetic studies in our laboratories demonstrated that the quantitative reactivity of X is incompatible with that expected for ·OH, and we suggested that, even for the classical Fenton reagent, this key oxidizing intermediate is likely to be an iron complex such as a coordinated peroxo species (16). Sawyer *et al.* (17) recently came to a similar conclusion after comparing relative reactivities of ·OH and Fenton-type oxidants toward several hydrocarbons *in a nonaqueous medium*, and some years ago Groves and Van Der Puy (18, 19) examined the stereoselectivity of cyclic alcohol oxidations by Fe^{2+}/H_2O_2 in acidic acetonitrile solutions and postulated a ferryl ($Fe{=}O^{2+}$) complex to be the key oxidant under their conditions. In the present study, we show that other substrates react with X in competition with NDMA; thus, the competitive quenching of Abs(A) provides a powerful spectrophotometric probe for the relative reactivities of various biologically relevant substrates with X. Furthermore, the presence of a second oxidizing intermediate (Y) in the sequence following reaction of Fe^{2+} with H_2O_2 is indicated by reaction patterns in the presence of $Ru(bpy)_3^{2+}$ (bpy = 2,2′-bipyridine), which acts as a selective quencher for Y. Thus, the present report demonstrates that the simple Fe^{2+}/H_2O_2 mixture in acidic aqueous solution generates at least two strongly oxidizing intermediates, neither of which shows the competitive reactivities expected for the hydroxyl radical.

EXPERIMENTAL

Warning! Most N-nitroso compounds are potent carcinogens and should be handled, stored, and discarded with due respect for their toxic nature.

Materials. NDMA and 30% hydrogen peroxide were purchased from Sigma. Perdeuterio NDMA ($NDMA\text{-}d_6$) was synthesized as described (20). Benzyl alcohol, dimethyl sulfoxide (DMSO), *t*-butanol, CH_3OH, C^2H_3OH, and $FeSO_4 \cdot 7H_2O$ were purchased from Aldrich.

Rate Studies. The kinetic experiments were performed using a Hi-Tech Scientific model SR-51MX multi-mixing stopped-flow spectrophotometer. Generally, the reactions were initiated by coinjecting into the reaction chamber an aqueous solution of NDMA plus $FeSO_4$ and H_2SO_4 from one syringe and an aqueous solution of H_2O_2 from a second syringe. Spectral changes were followed at selected wavelengths, and observed rate constants were computed from segments of the resulting absorbance vs. time curves. Data reduction was facilitated by the use of the Hi-Tech IS-1.0 RAPID KINETICS software, which uses an exponential fitting suite to determine first-order rate constants. All reactions were carried out at 22 ± 1°C. Quenching studies were carried out in a similar manner with various concentrations of the appropriate quencher added to the NDMA solution.

Reactions of the Fenton reagent with $Ru(bpy)_3^{2+}$ were studied by stopped-flow techniques by mixing a solution of Fe^{2+} plus $Ru(bpy)_3^{2+}$ in one syringe with a solution of H_2O_2 in the second syringe to give reaction solutions with the initial

The publication costs of this article were defrayed in part by page charge payment. This article must therefore be hereby marked "*advertisement*" in accordance with 18 U.S.C. §1734 solely to indicate this fact.

Abbreviations: NDMA, *N*-nitrosodimethylamine; bpy, 2,2′-bipyridine; DMSO, dimethyl sulfoxide; Abs(A), transient absorbance of species A.

concentrations $[Fe^{2+}]_i$ = 1.0 mM, $[Ru]_i$ = 0.5 mM (pH 1.7), $[H_2O_2]_i$ = 10–100 mM. Reactions were followed spectrophotometrically at 570 nm.

Optical spectra were recorded on a Hewlett-Packard model 8451 UV-visible diode array spectrophotometer.

Control Reactions. The nonreactivity of NDMA with Fe^{2+}, Fe^{3+}, or H_2O_2 individually was established by mixing acidic solutions of the components pairwise in separate cuvettes and recording the resulting electronic spectra. The stable nitrosyl species $Fe(H_2O)_5NO^{2+}$ was prepared *in situ* by mixing deaerated solutions of 0.005 M $FeSO_4$ and NO (saturated) (pH_{final} = 2.2). The resulting species displayed absorption bands at 450 and 580 nm in agreement with the literature (21).

Product Analyses. Stock solutions were prepared in deaerated aqueous solution. One set of solutions contained NDMA at various concentrations and either 40 mM or 10 mM H_2O_2. The other set contained either 10 mM or 2 mM $FeSO_4$ at pH 2.2. The reaction was initiated by mixing together 1.0-ml aliquots of each. After 30 s, a 0.4-ml portion of MeOH or 0.5 M NaOH was added to quench the reaction and precipitate any ferric ion. The solutions were filtered through a nylon 66 micropore syringe filter or centrifuged to remove the precipitated iron. The solutions were then assayed for NO_3^-/NO_2^- as described (20).

RESULTS AND DISCUSSION

Kinetics Studies: Reaction with NDMA. Mixing an acidic aqueous solution of $FeSO_4$ and NDMA with aqueous H_2O_2 via the stopped-flow technique (initial net concentrations: $[Fe^{2+}]_i$ = 5 mM, $[H_2O_2]_i$ = 20 mM, $[NDMA]_i$ = 100 mM, pH 2.1) led to the generation and decay of a transient absorbance, Abs(A) (Fig. 1), attributed to formation of a new species A (16). The spectrum of A displayed λ_{max} at 450 nm and 580 nm (relative absorbances 1.0 and 0.3) and was nearly identical to that of the $Fe(H_2O)_5NO^{2+}$ ion in acidic solution (21). Observed pseudo-first-order rate constants for the appearance and disappearance of A (followed at the monitoring wavelength, 625 nm) were each found to be independent of $[NDMA]_i$ but linear with respect to $[H_2O_2]_i$. From these data, the respective second-order rate constants k_{app} = 320 ± 40 $M^{-1}\cdot s^{-1}$ and k_{dis} = 107 ± 10 $M^{-1}\cdot s^{-1}$ were determined. Notably, the rate constant k_{app} for appearance of A is about 4-fold larger than that determined for Fe^{2+} oxidation to Fe^{3+} by H_2O_2 in the absence of NDMA (75 $M^{-1}\cdot s^{-1}$) (16). Since the formation, not the secondary reactions, of the putative ·OH intermediate would be the rate-limiting step in such oxidations, the substrate-dependent rate constants argue strongly against the intermediacy of the hydroxyl radical under these conditions (16).

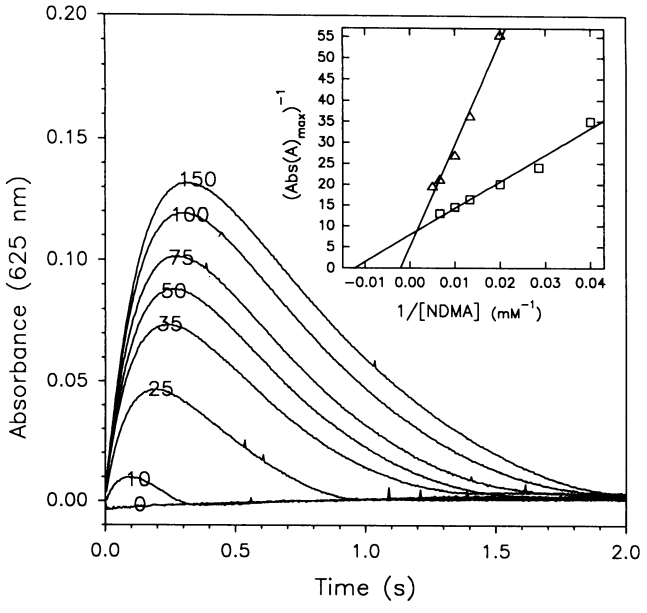

FIG. 1. Temporal absorbance changes at 625 nm for [NDMA] = 5, 10, 25, 35, 75, 100, and 150 mM where $[Fe^{2+}]$ = 5 mM and $[H_2O_2]$ = 20 mM. (*Inset*) Plots of $(Abs(A)_{max})^{-1}$ vs. $[NDMA]^{-1}$ (□; slope = 638 mM, x_{int} = 0.012 mM^{-1}, y_{int} = 7.9) and of $(Abs(A)_{max})^{-1}$ vs. $[NDMA\text{-}d_6]^{-1}$ (△; slope = 2447 mM, x_{int} = 0.0021 mM^{-1}, y_{int} = 5.05). From the relative x_{int} values, a kinetic isotope effect k_2^h/k_2^d of 3.6 can be estimated.

The maximum temporal absorbance $(Abs(A)_{max})$ for a specific experiment is a linear function of $[Fe^{2+}]_i$ at fixed $[H_2O_2]_i$ and $[NDMA]_i$ (both in excess). Furthermore, the plot of $(Abs(A)_{max})^{-1}$ vs. $[NDMA]_i^{-1}$ is linear (Fig. 1) and gives a K_m value of 88 ± 12 mM [$K_m = -(x_{int})^{-1}$, where x_{int} is the x-axis intercept, see below]. This behavior is consistent with the mechanism illustrated in Scheme I, in which the intermediate X is formed reversibly via reaction of Fe^{2+} with H_2O_2

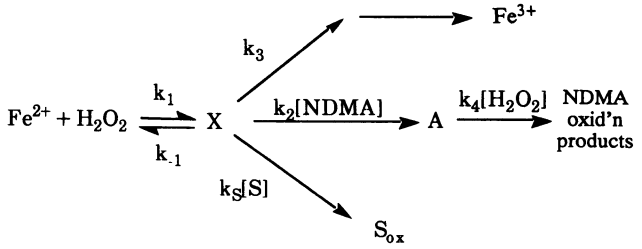

Scheme I

and then is depleted by competing unimolecular decay (k_3) and second-order (k_2) processes (16). In this context, the K_m value determined from Fig. 1 represents the $[NDMA]_i$, the concentration for which half of X is intercepted by NDMA rather than undergoing spontaneous decay (i.e., the condition where $k_2[NDMA] = k_3$).

When the stopped-flow experiments were carried out in the presence of added methanol (initial net concentrations: $[Fe^{2+}]_i$ = 0.5 mM, $[H_2O_2]_i$ = 20 mM, $[NDMA]_i$ = 200 mM), the magnitude of $Abs(A)_{max}$ at 450 nm was observed to decrease significantly with increasing MeOH concentration. A new absorption band at λ_{max} = 500 nm, representing a long-lived uncharacterized product, also resulted, but over a longer time period than that for formation of A. The plot of $(Abs(A)_S)^{-1}$ vs. [MeOH] (where $Abs(A)_S$ is the Abs(A) at 450 nm at a fixed time interval Δt = 0.5 s in the presence of a specified concentration of the substrate MeOH) proved to be linear and gave K_i = 43 ± 5 mM (Fig. 2*A*) [$K_i = -(x_{int})^{-1}$].

In the context of the model described in Scheme I, the K_i value represents that concentration of a substrate S (i.e., methanol in the above example) for which half the Abs(A) expected for a specified NDMA concentration is quenched—i.e., when $k_S[S] = k_2[NDMA]$ (actually, when $k_S[S] = k_2[NDMA] + k_3$, but at 200 mM NDMA, $k_2[NDMA] \gg k_3$). Thus, when that condition is met, one can accurately determine the ratio of rate constants $k_S/k_2 = [NDMA]/K_i$ for the relative reactivity of a substrate (e.g., MeOH) in competition with NDMA toward the oxidizing intermediate X without knowing the absolute values of the specific rate constants. Alternatively, one can determine the relative values of two different substrates. Thus for [NDMA] = 200 mM, the K_i(MeOH) value of 43 nm gives a k_2/K_S ratio of 5. According to this scheme, K_i(S) should be a function of $[NDMA]_i$; thus, it is reassuring to note that, for an analogous experiment with [NDMA] = 100 mM, K_i(MeOH) was determined to be 20 ± 4 mM (Fig. 2*A*), giving an identical k_2/k_S ratio (i.e., 5) to that found for 200 mM NDMA.

Similar quenching of Abs(A) was demonstrated when other substrates S were added to the Fe^{2+}/H_2O_2/NDMA system described above, and this technique was used to probe the relative reactivities of a catalog of organic and biologically relevant substrates. Plots of $(Abs(A)_S)^{-1}$ vs. [S] give values for $K_i(S)$, which therein provide a measure of the relative abilities for different S to compete with NDMA for X. For example, when the deuterated methanol C^2H_3OH was used as the substrate and [NDMA] = 200 mM, $K_i(C^2H_3OH)$ was determined to be 116 ± 20 mM. Comparison to the value determined for CH_3OH gives a kinetic isotope effect k_S^h/k_S^d = 2.7 ± 0.5 for the reaction of these two substrates with X. Similarly, the results reported in Table 1 are a collection of such $K_i(S)$ values for different substrates examined for the standard conditions $[Fe^{2+}]$ = 0.5 mM, H_2O_2 = 20 mM, [NDMA] = 200 mM.

Table 1 also lists rate constants (k_{OH}) that have been previously determined for the aqueous solution reactions of the same substrates with authentic hydroxyl radical generated by pulse radiolysis (22) and the relative reactivities of these normalized to the k_{OH} value for NDMA. Comparison of the k_S/k_2 ratios to the $k_{OH}(S)/k_{OH}(NDMA)$ ratios in Table 1 shows that, while there are some superficial similarities, the two patterns are quite distinct. One important observation is that the range of reactivities indicated by the k_S/k_2 ratios is considerably larger, a clear indication that the oxidizing intermediate that is a precursor to A (i.e., X) is more selective than is ·OH. It is apparent from these data that examination of only a limited number of substrates might have led one to conclude that the reactivity patterns of X and of ·OH are similar. However, such an interpretation does not hold true when one examines a more extensive list, such as that in Table 1. These competitive reactivities substantiate our earlier conclusion, based on the kinetics for Fenton reagent oxidation of NDMA (16), that the intermediate X must be a metal-containing oxidant formed by the reaction of Fe^{2+} with H_2O_2—i.e., *that X is not ·OH.*

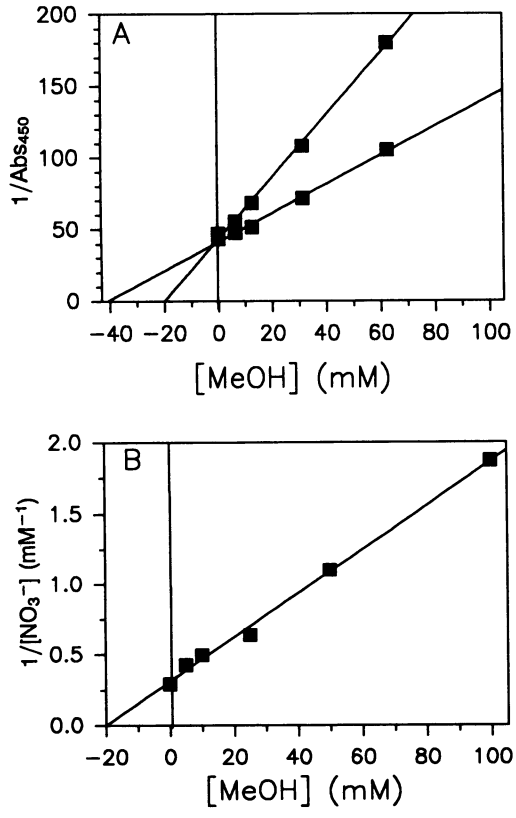

FIG. 2. (*A*) Plot of $(Abs(A)_S)^{-1}$ vs. [MeOH] for the conditions $[Fe^{2+}]$ = 0.5 mM, $[H_2O_2]$ = 20 mM, [NDMA] = 200 mM; K_i (i.e., $-x_{int}^{-1}$) 43 ± 5 mM. (*B*) Plot of $[NO_3^-]^{-1}$ vs. [MeOH] for $[Fe^{2+}]$ = 5 mM, $[H_2O_2]$ = 20 mM, [NDMA] = 100 mM, where the slope is 0.35 and y_{int} = 1.37 mM^{-1}.

NDMA Oxidation Product Studies. Chromatographic analysis of solutions resulting from the Fe^{2+}/H_2O_2 oxidation of NDMA showed the products to be CH_2O, CH_3NH_2, and NO_x^- ($NO_x^- \approx 90\%\ NO_3^-/10\%\ NO_2^-$), in agreement with Heur *et al.* (20).

$$(CH_3)_2NNO \xrightarrow{Fe^{2+}/H_2O_2} CH_2O + CH_3NH_2 + NO_3^-/NO_2^-$$

The $CH_2O/CH_3NH_2/NO_x^-$ ratio was determined to be 1:1:1 for $[NDMA]_i$ = 1, 10, or 100 mM with $[H_2O_2]_i$ = 20 mM and $[Fe^{2+}]_i$ = 5 mM. Although product ratios remained constant, total NO_x^- was found to increase in a nonlinear response to $[NDMA]_i$. The limiting yield of NO_x^- was determined as 4.7 mM from the inverse *y* intercept of the linear $[NO_x^-]^{-1}$ vs. $[NDMA]_i^{-1}$ plot ($[NDMA]_i$ from 25 to 200 mM). This value is, within experimental uncertainty, equal to $[Fe^{2+}]_i$ and is consistent with Scheme I—i.e., a mechanism by which all X is intercepted by NDMA under limiting conditions.

Table 1. Comparison of selectivities of intermediate X versus ·OH toward amino acids, nucleic acid components, and other substrates (S)

Substrate	$K_i(S)$,* mM	k_S/k_2†	$k_{OH}(S) \times 10^{-8}$,‡ ($M^{-1}s^{-1}$)	$k_{OH}(S)_{rel}$§
Miscellaneous				
NDMA		1.0	3.4	1.0
MeOH	43 ± 5	5	9.8	2.9
t-BuOH	28 ± 5	7	6.0	1.8
BzOH	0.8 ± 0.2	270	84	25
DMSO	2.8 ± 0.5	72	100	29
Bases				
Thymine	4 ± 1	50	54	16
Cytosine	6 ± 2	33	56	16
Adenine	8 ± 2	25	9	3
Sugars				
Deoxyribose	8 ± 1	25	25	7
Ribose	6 ± 1	33	15	4
Nucleosides				
Thymidine	3 ± 0.5	67	46	14
dC	7 ± 0.5	29	60	18
dA	26 ± 3	8	3	10
Nucleotides				
dCMP	6 ± 1	33	30	9
dAMP	16 ± 2	13	14	4
dGMP	7 ± 1	29	46	14
Amino acids				
Serine	≈100	≈2	≈3.2	1
Valine	30 ± 3	7	8.6	2.5
Arginine	31 ± 3	7	6.7	2
Lysine	23 ± 2	9	7.7	2
Histidine	10 ± 2	20	19	5.5
Phenylalanine	2 ± 0.5	100	65	19
Tryptophan	3 ± 0.2	70	110	32
Tyrosine	3 ± 0.5	70	120	38

BzOH, benzyl alcohol.

*$K_i(S) = -x_{int}$ of $(Abs(A)_S)^{-1}$ vs. [S] plots (where $Abs(A)_S$ is the absorbance due to formation of A determined at 450 nm at a fixed time interval Δt = 0.5 s for a specified [S], $[Fe^{2+}]$ = 0.5 mM, $[H_2O_2]$ = 20 mM, [NDMA] = 200 mM). This represents the concentration of S required to quench 50% $Abs(A)_{max}$.

†Ratio of relative rate constants for trapping of X by S or by NDMA as described in the text.

‡Second-order rate constants for the reaction of each substrate with OH· (ref 24).

§$k_{OH}(S)_{rel} = k_{OH}(S)/k_{OH}(NDMA)$.

Addition of MeOH sharply suppressed formation of NO_x^- products when the oxidations were carried out with the initial concentrations $[Fe^{2+}]_i$ = 5 mM, $[H_2O_2]_i$ = 20 mM, and $[NDMA]_i$ = 100 mM. Under these conditions, the linear plot of $[NO_x^-]^{-1}$ vs. [MeOH] (Fig. 2*B*) gave a K_i value of 20 ± 4 mM, the same as that found for MeOH quenching of the formation of transient A for $[NDMA]_i$ = 100 mM (Fig. 2*A*). Thus, the correspondence between the K_i values for quenching of A formation determined spectrally and of NO_x^- product yields determined by chromatography indicated that A is a precursor to the NDMA oxidation products.

Reaction with Ru(bpy)$_3^{2+}$. This reaction ([Ru] = 0.5 mM) with Fenton reagent (0.5 mM Fe^{2+} and 20 mM H_2O_2) leads to rapid formation of a new species [Ru_{ox}, possibly a ligand-oxidized product (23)] with a λ_{max} at 540 nm. Kinetics studies (monitoring wavelength = 570 nm) over a range of H_2O_2 concentrations obeyed the rate law:

$$\frac{d[Ru_{ox}]}{dt} = k' [Fe(II)] [H_2O_2]$$

with a second-order rate constant k' = 74 ± 20 $M^{-1}\cdot s^{-1}$, which was experimentally indistinguishable from that (75 $M^{-1}\cdot s^{-1}$) determined for the oxidation of Fe^{2+} to Fe^{3+} under these conditions. With $[Fe^{2+}]_i$ = 0.5 mM, the magnitude and rate of the absorbance change at 540 nm (attributed to Ru_{ox} formation) both proved independent of the initial Ru concentration over the range 0.5–5 mM. Thus, we conclude that the oxidation of Ru(bpy)$_3^{2+}$ to Ru_{ox} occurs subsequent to the rate-limiting unimolecular decay of X, a process that leads to ferric ion formation in the absence of other substrates (the k_3 step in Scheme I). Since Fe^{3+} itself does not oxidize Ru(bpy)$_3^{2+}$, one is thus led to conclude that the latter must be intercepting a second oxidizing intermediate, Y, which appears subsequent to X but prior to Fe^{3+}. This proposal is illustrated in Scheme II.

This reaction provides an additional spectrophotometric/kinetic probe of the Fenton reaction. Addition of the various substrates S shown above to intercept X resulted in S concentration-dependent quenching of Ru_{ox} formation as monitored at 570 nm ($[Ru]_i$ = 0.5 mM, $[Fe^{2+}]_i$ = 0.5 mM, $[H_2O_2]_i$ = 20 mM, pH = 1.7, $[S]_i$ = 0–20 mM). Plots of $(Abs(Ru_{ox}))^{-1}$ vs. [S] [where $Abs(Ru_{ox})$ is the absorbance at 570 nm after Δt = 5 s] each proved to be linear, and $K_i'(S)$ values for these quenching experiments (Table 2) were again determined from the $-x_{int}$ values as described above (23).

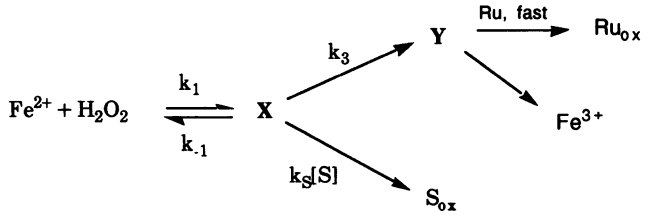

Scheme II

According to the model described in Scheme II, the trapping of X by S will inhibit formation of Y by the unimolecular k_3 pathway. Since the latter step is rate-limiting in formation of Ru_{ox}, the $K_i'(S)$ values determined in this case represent substrate concentrations when $k_S[S] = k_3$.

Table 2 compares $K_i(S)$ values normalized to that for S = MeOH as determined for quenching of Ru(bpy)$_3^{2+}$ oxidation to analogous values for quenching of the formation of A. While there is some variation between the two series, the observed patterns are quite similar; indeed, the differences might well be attributable to the experimental uncertainties (as large as ±25%) in these extrapolated K_i terms. Thus, the comparable reactivity patterns indicate a common mechanism for both quenching processes, consistent with the commonality being the interception of X in each case. This conclusion is reinforced by the observation that K_i'(MeOH) is (within ±20% experimental uncertainty) unaffected by increasing the Ru concentration from 0.5 to 2.0 mM.

Table 2. Summary of $K_i'(S)$ values for the quenching of Ru(bpy)$_3^{2+}$ oxidation by Fe^{2+}/H_2O_2 in acidic aqueous solution and a comparison of relative $K_i'(S)$ values with those for quenching of NDMA oxidation

Substrate	$K_i'(S)$,* mM	$K_i'(S)_{rel}$†	$K_i(S)_{rel}$‡
Alcohols			
MeOH	14 ± 3	1.0	1.0
BuOH	14 ± 3	1.0	0.65
Deoxyribose	3.6 ± 0.6	0.26	0.19
Nucleosides			
Thymidine	1.3 ± 0.3	0.09	0.07
dC	3.0 ± 0.6	0.21	0.16
dA	1.8 ± 0.4	0.13	0.19
Nucleotides			
dCMP	1.0 ± 0.3	0.07	0.14
dGMP	0.8 ± 0.2	0.06	0.16
Amino acids			
Valine	16 ± 0.4	1.1	0.70
Arginine	12 ± 3	0.86	0.72
Lysine	12 ± 3	0.86	0.54
Histidine	6.2 ± 1.5	0.44	0.23
Tryptophan	1.6 ± 0.4	0.11	0.07

The conditions were $[Ru]_i$ = 0.5 mM, $[Fe^{2+}]_i$ = 0.5 mM, $[H_2O_2]_i$ = 20 mM, pH = 1.7, $[S]_i$ = 0–20 mM.

*$K_i(S) = -x_{int}$ of $(Abs(Ru_{ox})_S)^{-1}$ vs. [S] plots (where $Abs(Ru_{ox})_S$ is the absorbance due to formation of Ru_{ox} determined at 570 nm at a fixed time interval Δt = 5 s in the presence of a specified [S]).

†$K_i'(S)_{rel} = K_i'(S)/K_i'(MeOH)$.

‡$K_i(S)_{rel} = K_i(S)/K_i(MeOH)$, where the $K_i(S)$ values are for substrate quenching of transient A formation as summarized in Table 1.

An obvious question is whether this second intermediate is ·OH or some other oxidant. This can again be addressed by considering the quenching by MeOH, which displayed a $K_i(S)$ value consistent with a mechanism operating by interception of X. The rate constants for the second-order reactions of MeOH and Ru(bpy)$_3^{2+}$ with ·OH have been determined to be 9.8×10^8 and 5×10^9 $M^{-1}\cdot s^{-1}$, respectively (24). Thus, if Y were ·OH, the condition necessary to quench half the oxidation of Ru would be met when $k_{OH}(MeOH)$ [MeOH] = $k_{OH}(Ru)$ [Ru]. Given that these experiments were carried out for $[Ru]_i$ = 0.5 mM, this condition would have been met for [MeOH] = 2.5 mM, which is much less than the 14 mM value observed. Thus, Y also cannot be ·OH.

SUMMARY

The above results indicate that two strongly oxidizing intermediates, denoted as X and Y, are formed in the oxidation of organic substrates by the simple mixture of ferrous ion and hydrogen peroxide in acidic aqueous solution. Furthermore, examination of the competitive reactivities of these intermediates, using the oxidations of NDMA and of Ru(bpy)$_3^{2+}$ as spectroscopic probes, shows that neither intermediate can be the hydroxyl radical. The reactivity patterns for X and Y differ from the known reactions of ·OH under comparable conditions; one feature is the much greater selectivities of these intermediates.

The exact natures of X and Y are as yet uncertain, although kinetic simulation studies carried out in this laboratory (16) suggest that X is formed by a reversible reaction of Fe^{2+} with H_2O_2. Thus, we consider a peroxo complex such as $Fe^{II}(OOH)$ to be a likely candidate for X. The substantial kinetic isotope

effects noted for the reaction of X both with MeOH-d_3 or NDMA-d_6 indicate that the rate-limiting steps with both substrates involve direct activation of a C—H bond, perhaps via hydrogen atom abstraction. Since Y appears to form via unimolecular decomposition of X, a likely candidate for Y would be an iron(IV) oxo complex. Both $Fe^{II}(OOH)$ and FeO^{2+} would be capable of one-electron redox reactions such as H atom abstraction, and it is easily imagined how such might be mistaken for ·OH, if a narrow range of substrates were examined for competitive reactivities. Ferryl and hydroperoxy complexes have been subjects of previous speculation regarding Fenton-type reagents under certain conditions, although concrete evidence for two oxidizing intermediates has not been described.

Fenton-type chemistry has been implicated in the oxidative processes involved in the etiology of many disease and degenerative states of organisms (2–10). Hydroxyl radicals are often invoked as being responsible for such damage; indeed the term "Fenton chemistry" is sometimes used to imply reactions involving free ·OH. The present study demonstrates by using the simplest [and original (1)] Fenton reagent that such descriptions are misnomers. Indeed the Fenton system is characterized by two oxidizing intermediates, neither of which is free ·OH. Each appears to be a metal-based oxidant, the reactivities of which should be considerably more selective and governed by local environments in biological systems than that of ·OH. The question one now must ask is whether the historical Fenton reagent is simply an inadequate model for *in vivo* metal-catalyzed oxidations by peroxide or if the importance of hydroxyl radical in such situations has been broadly overestimated.

We thank Dr. Larry Keefer of the Laboratory of Comparative Carcinogenesis for advice, support, and comments. Partial support from National Science Foundation Grant CHE-9024845 to P.C.F. is gratefully acknowledged.

1. Fenton, H. J. H. (1894) *J. Chem. Soc.* **65**, 899–910.
2. Ames, B. N., Cathcart, R., Schwiers, E. & Hochstein, P. (1981) *Proc. Natl. Acad. Sci. USA* **78**, 6858–6862.
3. Halliwell, B. & Gutteridge, J. M. C. (1986) *Arch. Biochem. Biophys.* **246**, 501–514.
4. Halliwell, B. & Gutteridge, J. M. C. (1984) *Biochem. J.* **219**, 1–14.
5. Aust, S. D., Morehouse, L. A. & Thomas, C. E. (1985) *Free Radicals Biol. Med.* **1**, 3–25.
6. Walling, C. (1975) *Acc. Chem. Res.* **8**, 125–131.
7. Sutton, H. C., Vile, G. F. & Winterbourn, C. C. (1987) *Arch. Biochem. Biophys.* **256**, 462–471.
8. Rush, J. D. & Koppenol, W. H. (1988) *J. Am. Chem. Soc.* **110**, 4957–4963.
9. Imlay, J. A., Chin, S. M. & Linn, S. (1988) *Science* **240**, 640–642.
10. Rahhal, S. & Richter, H. W. (1988) *J. Am. Chem. Soc.* **110**, 3126–3133.
11. Haber, F. & Weiss, J. J. (1934) *Proc. R. Soc. London Ser. A* **147**, 332–351.
12. Bray, W. C. & Gorin, M. H. (1932) *J. Am. Chem. Soc.* **54**, 2124–2125.
13. Merz, J. H. & Waters, W. A. (1947) *Discuss. Faraday Soc.* **2**, 179–187.
14. Merz, J. H. & Waters, W. A. (1949) *J. Chem. Soc.* **S15**, 2427—2433.
15. Cahill, A. E. & Taube, H. (1952) *J. Am. Chem. Soc.* **74**, 2312–2318.
16. Wink, D. A., Nims, R. W., Desrosiers, M. F., Ford, P. C. & Keefer, L. K. (1991) *Chem. Res. Toxicol.* **4**, 510–512.
17. Sawyer, D. T., Kang, C., Liobet, A. & Redman, C. (1993) *J. Am. Chem. Soc.* **115**, 5817–5818.
18. Groves, J. T. & Van Der Puy, M. (1974) *J. Am. Chem. Soc.* **96**, 5274–5275.
19. Groves, J. T. & Van Der Puy, M. (1975) *J. Am. Chem. Soc.* **97**, 5290–5297.
20. Heur, Y.-H., Streeter, A. J., Nims, R. W. & Keefer, L. K. (1989) *Chem. Res. Toxicol.* **2**, 247–253.
21. Epstein, I. R., Kustin, K. & Warshaw, J. (1980) *J. Am. Chem. Soc.* **102**, 3751–3758.
22. Wink, D. A. & Desrosiers, M. F. (1991) *Radiat. Phys. Chem.* **38**, 467–472.
23. Neta, P., Silverman, J., Markovic, V. & Rabani, J. (1986) *J. Phys. Chem.* **90**, 703–707.
24. Buxton, G. V., Greenstock, C. L., Phillip, W. & Ross, A. B. (1988) *J. Phys. Chem. Ref. Data* **17**, 513–886.